Bimorph micro heat engines based on carbon nanotube freestanding films

To cite this article: Takashi Ikuno *et al* 2015 *Appl. Phys. Express* **8** 115101

OPEN ACCESS

Applied Physics Express 8, 115101 (2015)
http://dx.doi.org/10.7567/APEX.8.115101

Bimorph micro heat engines based on carbon nanotube freestanding films

Takashi Ikuno, Tatsuo Fukano, Kazuo Higuchi, and Yasuhiko Takeda

Toyota Central R&D Labs., Nagakute, Aichi 480-1192, Japan
E-mail: TIkuno@mosk.tytlabs.co.jp

Received August 26, 2015; accepted September 13, 2015; published online October 5, 2015

We have found that lightweight bimorph strips consisting of multiwalled carbon nanotube freestanding films (MWNT-FSFs) and Ni thin films exhibit a continuous bending–stretching motion on a hot plate even below the temperature of 100 °C in an environment at room temperature. In fact, the Ni/MWNT-FSFs exhibited this motion at a temperature difference of as small as 5 °C. The requirements of this motion have been qualitatively elucidated by a simulation based on a relaxation time approximation. © 2015 The Japan Society of Applied Physics

Harvesting large amounts of low-temperature heat wasted from industrial processes, residential buildings, and even human bodies is an important subject aimed at the development of micro power sources, sensors, and actuators for wireless-sensor network devices,[1] although it has been rarely claimed because of the second law of thermodynamics.[2] In addition to thermoelectric (TE) energy harvesters utilizing the Seebeck effect,[1] other TE devices that are composed of heat engines (HEs), which turn thermal gradients into mechanical energy, and mechanical-to-electric (M-to-E) transducers[3–5] (piezoelectric, electret, and tribo-electric devices) have recently attracted attention because their output voltages are higher than those of the Seebeck devices.[1,2] In particular, reducing the size, weight, and operating temperature with respect to room temperature (RT), ΔT, of HEs is required for their integration into microdevices. For this purpose, diaphragm-like HEs, in which thin plates that exhibit temperature-dependent distortion are placed between opposed hot and cold plates, have been proposed and created.[2] However, further reductions in size and weight are needed, since these HEs include large heat sinks.[2]

On the basis of these diaphragm-like HEs, we propose fundamentally different lightweight bimorph HEs using carbon nanotube (CNT) freestanding films (FSFs) in this study. A CNT has an extremely small coefficient of thermal expansion (CTE).[6] When one side of a CNT-FSF is coated with a different material, the CTE of which is larger than that of the CNT, the ensemble behaves as a lightweight bimorph. A lightweight strip-shaped bimorph is supposed to show a continuous bending–stretching motion without a heat sink. A possible mechanism for the motion is as follows: First, when the lightweight strip-shaped bimorph is placed on the surface of a hot plate, it bends into a curved shape (convex upward). Second, the upper part of the curved bimorph is quenched because the lightweight bimorph has a low heat capacity, whereas the lower part near the hot plate is still at a high temperature, resulting in an increase in curvature. Third, the curvature radius of the curved bimorph decreases because the temperature of the upper part is increased again. Then, the second and third actions are repeated, resulting in a continuous bending–stretching mechanical motion, like an inchworm.[7]

In this study, we describe the fabrication of the CNT-FSF-based lightweight bimorph and experimental verifications of the mechanical motion without a heat sink. The fabricated

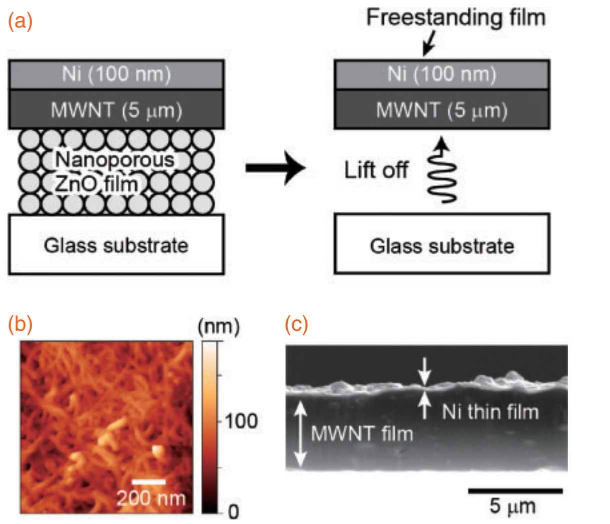

Fig. 1. (a) Synthesis method for Ni/MWNT freestanding films. After the deposition of the ZnO nanoporous film, MWNT film, and Ni thin film, the ZnO film was dissolved; thus, a Ni/MWNT freestanding film was obtained. (b) Atomic force microscope image of the MWNT film after the spray coating of MWNTs. (c) Cross-sectional scanning electron microscope image of the Ni/MWNT freestanding film.

bimorph strip showed a continuous bending–stretching motion on a hot plate at a constant temperature of even less than 100 °C. Moreover, the requirements of the motion were revealed through simulation.

We used a Ni thin film and a multiwalled CNT (MWNT)-FSF for the bimorph HE. The CTE of Ni is 12.8×10^{-6}/K,[8] which is significantly larger than that of a MWNT.[6] Figure 1(a) shows the fabrication method for the Ni/MWNT-FSF. First, a flat glass substrate was cleaned in ethanol and acetone. Second, a ZnO nanoparticle sacrificial layer was deposited on the glass substrate by the doctor blade method,[9] using a paste that includes ZnO nanoparticles of 20–30 nm diameter. Because this ZnO layer contains many pores, it is easily dissolved during the lift-off process described below. Third, an approximately 5-μm-thick MWNT film was deposited by a spray coating method at the substrate temperature of 120 °C. A MWNT ink purchased from Meijo Nano Carbon for the spray coating included MWNTs (0.2 wt%), with a diameter ranging from 10 to 40 nm, in an aqueous solution. We confirmed the surface morphology of the deposited film using an atomic force microscope (Hitachi

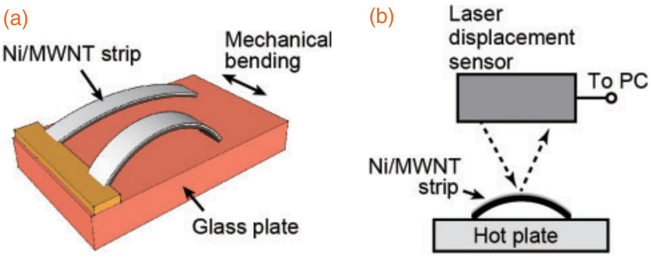

Fig. 2. (a) Schematic of the Ni/MWNT-FSF device that exhibits a bending–stretching motion. (b) Schematic of the experimental setup for measuring the time evolution of the motion. T_s is the temperature of the hot plate.

High-Tech Science E-sweep), as shown in Fig. 1(b). Most of the MWNTs were entangled in the film plane; standing MWNTs were rarely observed. Fourth, a 100-nm-thick Ni thin film was deposited on the MWNT film by radio-frequency magnetron sputtering at RT. Finally, the ZnO layer was removed with hydrochloric acid (0.1 M), and the FSF was obtained, as shown in Fig. 1(a). Figure 1(c) shows a typical scanning electron microscope image of the resultant Ni/MWNT-FSF. Although the surface morphology of the MWNT-FSF was rough, the Ni thin films uniformly covered the surface of the MWNT-FSF. We confirmed that the density per unit area of the Ni/MWNT-FSF was 550 μg/cm^2.

After synthesizing the bimorph FSF, we reshaped it into a strip structure approximately 2×10 mm^2 in size for the observation of the mechanical motion by heating. The obtained Ni/MWNT-FSF strips showed a curved shape with a curvature radius of 3.8 mm at RT. The curvature at RT was probably due to the existence of stresses at the Ni/MWNT interface caused by the difference in CTE and/or the existence of internal stress in the Ni thin film, which is caused by fabrication processes such as sputtering.

Then, the Ni/MWNT strip was placed on a flat glass plate (Matsunami Glass S1111) in such a manner that its MWNT plane faced the glass plate, as shown in Fig. 2(a). When the glass with the bimorph strip was installed on a hot plate, it immediately started to show the bending–stretching mechanical motion. The height of the curved strip during the mechanical motion was monitored by a laser displacement sensor (Keyence LJ-V7080), as shown in Fig. 2(b).

Figure 3(a) shows the time evolution of the maximum height of the Ni/MWNT strip and a histogram of the height as functions of the temperature of the hot plate. At 29 °C, which was higher than RT by 2 °C, there was no mechanical motion. At 32 °C, we observed that the mechanical motion started. The peak-to-peak height (h_{pp}) was approximately 0.02 mm. Even at body temperature (approximately 36 °C), the bimorph strip clearly showed the mechanical motion. At 100 °C, h_{pp} exceeded 0.1 mm. With increasing temperature, both the frequency and amplitude of the motion increased. The numbers of peaks during 60 s at temperatures of 40, 60, and 100 °C were approximately 30, 70, and 90, respectively. No periodic oscillations were observed. The histogram showed a couple of peaks over 36 °C, indicating that there were two stable states of the shapes during the heating. A movie of the motion is shown in the online supplementary data at http://stacks.iop.org/APEX/8/115101/mmedia. The micro HE in the movie is a Ni/MWNT strip (4×10 mm^2) on a highly oriented pyrolytic graphite sheet, which was operated at 120 °C. Another micro HE, a compound semiconductor (Cu_2ZnSnS_4) thin film/MWNT strip, is also shown in the movie.

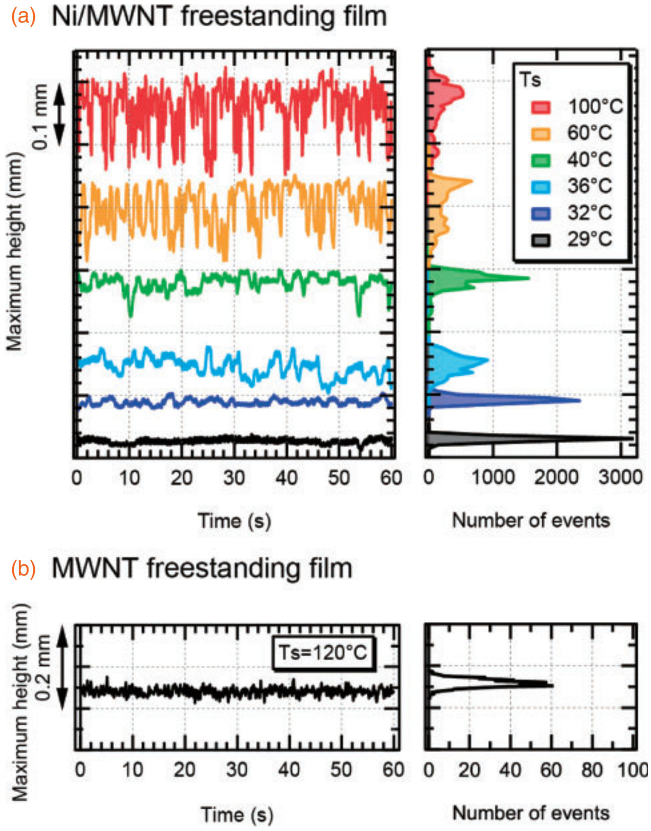

Fig. 3. Time evolution of the maximum height and histogram of the height for (a) Ni/MWNT-FSF and (b) MWNT-FSF.

In addition, to confirm the need for the bimorph structure, we investigated the thermal actuation of a MWNT-FSF without a Ni thin film. Figure 3(b) shows the time evolution of the maximum height of the MWNT strip (2×10 mm^2) at 120 °C. No notable mechanical motion was observed even at a temperature higher than the operating temperatures of the bimorph strips. Thus, we found that the existence of a thin film whose CTE is higher than those of MWNTs on one side of the MWNT-FSF (i.e., a bimorph structure) is required for the bending–stretching motion on a heat source. It was also confirmed that this motion is not caused solely by the convection around the surface of a hot plate.

The Ni/MWNT strip exhibited the continuous bending–stretching mechanical motion even at a temperature difference of 5 °C. Compared with other diaphragm-like HEs in terms of the operating temperature T_s and ΔT, those of our Ni/MWNT-FSFs are comparable to or lower than those of other HEs. The T_s and ΔT of a shape-memory-alloy-based HE are 100 and 52 °C, respectively.[2] A thermomagnetic generator showed T_s of 32 °C and ΔT of 18 °C.[10] A curved bimetallic HE operated at T_s of 47 °C and ΔT of 5 °C.[4] A remarkably different feature from other micro HEs mentioned above is the fact that our bimorph HEs do not need heat sinks. This is a great advantage for downscaling device ensembles and realizing stand-alone actuators.[7]

Next, we investigated the mechanical response of the Ni/MWNT-FSF by applying thermal energy from a laser. The inset of Fig. 4 shows the experimental setup. One end of a

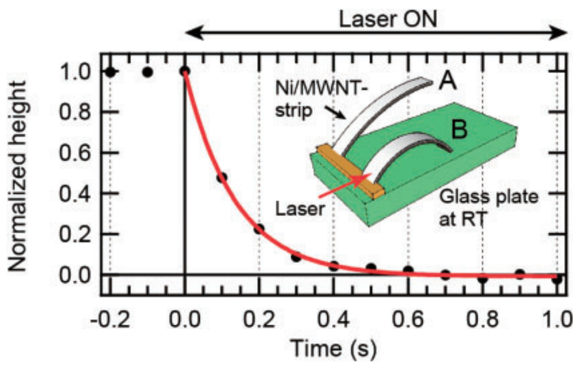

Fig. 4. Time evolution of the height change during laser irradiation ($\lambda = 785$ nm). The height was normalized by the height of the initial shape. The response time was approximately 0.14 s.

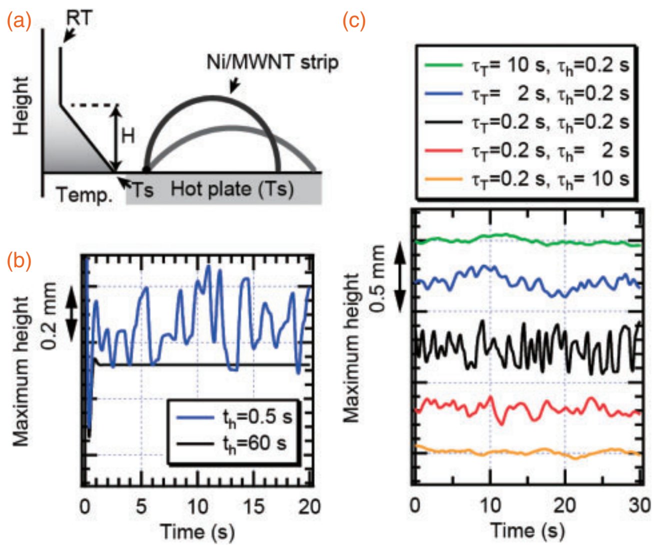

Fig. 5. (a) Schematic of the simulation model of the bending–stretching motion. (b) Time evolution curves of the maximum heights when t_h values are 0.5 and 60 s. (c) Time evolution curves of the maximum heights for various τ_T and τ_h values.

Ni/MWNT strip is fixed on a glass plate and the other is separated from the plate (shape A in the inset of Fig. 4). When the strip is irradiated by a laser, the local temperature increases and the shape should change to shape B. We used a semiconductor laser with a wavelength of 785 nm and a power of 30 mW. The laser beam was focused on the strip; the spot size was less than 100 µm. Figure 4 shows the height normalized by the initial value as a function of the elapsed time after the laser irradiation started. At approximately 2 ms, an initial mechanical motion was observed (data not shown in this paper). After that, the strip showed an equilibrium shape with a time constant of 0.14 s, which was estimated from the fitting of the time evolution with a single exponential curve, as shown in Fig. 4. A possible reason why the initial mechanical response is very fast is that the heat capacity of our FSF is small owing to its low weight. It is likely that the low thermal conductivity of the FSF determines the time at which it takes the equilibrium shape. We confirmed that (1) the FSF shows initial motion several ms after obtaining thermal energy, and (2) the FSF reaches thermal equilibrium less than 1 s after the laser irradiation starts.

On the basis of the experimental results, we performed a simulation study to investigate the operating conditions of the bending–stretching motion on the hot plate at a constant temperature. Figure 5(a) shows a schematic of the simulation model. We defined the temperature gradient from the temperature of the hot plate ($T = T_s$) and the environmental temperature ($T = \mathrm{RT}$) around the surface of the hot plate. The height H at which the temperature becomes RT can be described as $H = \lambda/\eta$, where λ is the thermal conductivity of air [$\lambda = 7 \times 10^{-5}\ T_s + 0.0237$ (W m^{-1} K^{-1})[11]] and η is the heat transfer coefficient of air. When the FSF is placed on the hot plate, it starts to bend because of increases in temperature and heat conduction through itself. We assumed that the time derivatives of the shape represented by the height distribution of the FSF [$h(x,t)$] and the temperature distribution of the FSF [$T(x,t)$] are described by the following equations based on a relaxation time approximation:

$$\frac{\partial h(x,t)}{\partial t} = -\frac{h(x,t) - h^{(\mathrm{eq})}(T(x,t))}{\tau_h}, \tag{1}$$

$$\frac{\partial T(x,t)}{\partial t} = -\frac{T(x,t) - T^{(\mathrm{eq})}(h(x,t))}{\tau_T}, \tag{2}$$

where x is the horizontal position, t is the time, $h^{(\mathrm{eq})}$ is the equilibrium height distribution of the FSF, τ_h is the relaxation time (namely, the time constant) of the shape change, $T^{(\mathrm{eq})}$ is the equilibrium temperature distribution of the FSF, and τ_T is the relaxation time of the FSF's temperature distribution. Heat transfer at the contact points between the FSF and the hot plate was neglected because the contact area is small for this experimental setup.

Furthermore, we introduced the effect of the natural convection around the hot plate surface. Since it is complex to express the convection mathematically, we assumed that H is maintained for a period of t_h and is decided for each period by η of a random number between 10 to 15.

We solved the simultaneous differential equations under the following parameters. The thickness and CTE of the Ni thin film were 100 nm and 12×10^{-6}/K, respectively, whereas those of the MWNT-FSF were 5 µm and 0.1×10^{-6}/K, respectively, since the axial CTE of a MWNT is approximately 0.[6] The length of the Ni/MWNT strip was 10 mm, and RT was 25 °C.

Figure 5(b) shows the simulation results of the maximum height of the Ni/MWNT-FSF during heating at $T_s = 100$ °C as a function of elapsed time. Because the time constant of the shape change was 0.14 s for the laser irradiation, as shown in Fig. 4, we adopted $\tau_T = 0.2$ s. The same value was used for τ_h. When t_h was 60 s (H is constant during the simulation), the bimorph strip showed bending and stretching at the initial stage, but the motion stopped after that. In contrast, when t_h was 0.5 s, it showed a continuous bending–stretching motion. Next, we investigated the effects of the relaxation times τ_T and τ_h on the motion. Figure 5(c) shows the simulation results calculated with various parameters. We found that the amplitude of the motion decreased with increasing τ_T and τ_h. Thus, the requirements for the motion were found to be (1) the fluctuation of ambient temperature around the hot plate and (2) short relaxation times for both the shape and the temperature distribution.

Because the Ni/MWNT-FSFs fabricated in this study are light, they respond sensitively to the ambient temperature.

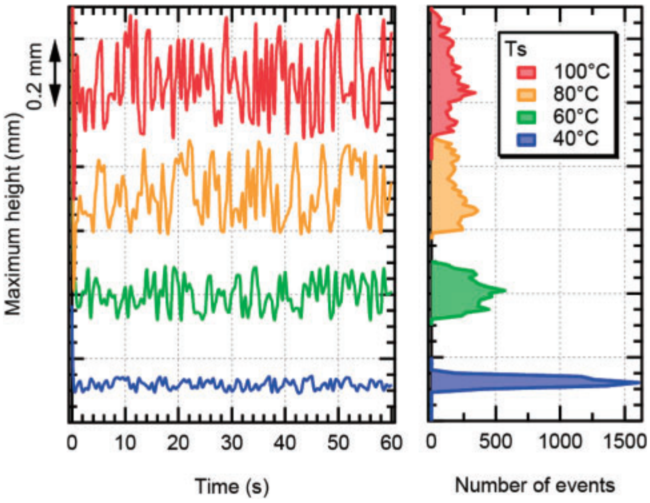

Fig. 6. Simulation results of the bending–stretching motion at various hot plate temperatures.

Moreover, the small CTE of MWNTs leads to a large displacement of the motion. To improve the response time of the motion, the thermal conductivity of the FSF should be increased by controlling the alignment of the MWNTs and by making better junctions between the MWNTs.

Figure 6 shows the simulation results as a function of T_s with $\tau_T = \tau_h = 0.2$ s. The amplitudes increased with T_s. This trend agrees with the experimental result shown in Fig. 3.

In conclusion, we fabricated bimorph micro HEs based on MWNT-FSFs. The Ni/MWNT-FSF strips showed the bending–stretching motions on a hot plate whose temperature was constant and even less than 100 °C. The requirements of the motion were revealed by the simulation based on the relaxation time approximation: (1) the fluctuation of ambient temperature around the hot plate, and (2) short relaxation times for both the shape and the temperature distribution. Although we used Ni thin films for realizing the micro HEs, a wide variety of materials having CTEs larger than those of MWNTs can be utilized for the application of these HEs. Moreover, if we couple M-to-E energy conversion devices with our micro HEs, electrical energy can be generated from thermal energy via mechanical motion.

In the research field of nanocarbons, no heat-driven actuators using CNTs that show continuous bending–stretching motion have been reported, although there are reports of a humidity-driven actuator using a bilayer of a MWNT film and a graphene oxide film,[12] an electric-driven actuator using a CNT film,[13] and an infrared-light-driven actuator using a CNT/polymer composite.[14] We believe that the MWNT-FSFs developed in this study could be one of the building blocks for energy conversion nanodevices.

Acknowledgment This work was partly supported by JSPS KAKENHI Grant Numbers 15K17448 and 60466331.

1) N. S. Hudak and G. G. Amatucci, J. Appl. Phys. **103**, 101301 (2008).
2) S. Percy, C. Knight, S. McGarry, A. Post, T. Moore, and K. Cavanagh, *Thermal Energy Harvesting for Application at MEMS Scale* (Springer, New York, 2014).
3) C. R. Bowen, H. A. Kim, P. M. Weaver, and S. Dunn, Energy Environ. Sci. **7**, 25 (2014).
4) A. Arnaud, S. Boisseau, S. Monfray, O. Puscasu, G. Despesse, J. Boughaleb, Y. Sanchez, F. Battegay, M. Fourel, S. Audran, F. Boeuf, J. Delamare, G. Delepierre, G. Pitone, and T. Skotnicki, J. Phys.: Conf. Ser. **476**, 012062 (2013).
5) S. Wang, L. Lin, Y. Xie, Q. Jing, S. Niu, and Z. L. Wang, Nano Lett. **13**, 2226 (2013).
6) Y. Maniwa, R. Fujiwara, H. Kira, H. Tou, E. Nishibori, M. Takata, M. Sakata, A. Fujiwara, X. Zhao, S. Iijima, and Y. Ando, Phys. Rev. B **64**, 073105 (2001).
7) W. Wang, J.-Y. Lee, H. Rodrigue, S.-H. Song, W.-S. Chu, and S.-H. Ahn, Bioinspiration Biomimetics **9**, 046006 (2014).
8) R. E. Taylor, *Thermal Expansion of Solids* (ASM International, Materials Park, OH, 1998).
9) D. Hotza and P. Greil, Mater. Sci. Eng. A **202**, 206 (1995).
10) M. Ujihara, G. P. Carman, and D. G. Lee, Appl. Phys. Lett. **91**, 093508 (2007).
11) N. B. Vargaftik, L. P. Filippov, A. A. Tarzimanov, and E. E. Totskii, *Handbook of Thermal Conductivity of Liquids and Gases* (CRC Press, Boca Raton, FL, 1993).
12) S. Park, J. An, J. W. Suk, and R. S. Ruoff, Small **6**, 210 (2010).
13) R. H. Baughman, Science **284**, 1340 (1999).
14) S. V. Ahir and E. M. Terentjev, Nat. Mater. **4**, 491 (2005).